STRENGTH OF POST-LIQUEFACTION FLOWS - A SPECULATIVE VELOCITY DEPENDANT MODEL

R.O. DAVIS
University of Canterbury, Christchurch, New Zealand

M.D. BOLTON
Cambridge University, Cambridge, UK

9th Int. Conf. of Int. Association for Computer Methods & Advances in Geomechanics, Wuhan, China, Nov 97

ABSTRACT: Many observations have shown that post-liquefaction flows exhibit enhanced mobility due to some form of partial fluidisation leading to more rapid motions and longer runout distances than might be otherwise expected. These phenomena may be explained by anticipating a reduction in frictional strength due to increasing velocity of flow. In this paper we investigate a simple model which manifests this effect. The model produces a rich variety of strength-velocity responses, including near complete loss of strength at high velocities.

INTRODUCTION

The aim of this paper is to construct a simple numerical model for flow of a saturated granular mass and to assess the effect of velocity on the average frictional strength at the interface between the flow and its bed. We are motivated by the need for a rational description for behaviour of post-liquefaction flows. Under certain circumstances these may potentially attain high velocities. Observations of velocities greater than 10 *m/s* are common, as are instances where flows have exhibited unexpectedly long run-out distances over relatively flat ground. Numerous examples of flow slides are described by Rouse (1984), Johnson (1984), Seed (1987), and Stark and Mesri (1992).

Estimation of post-liquefaction soil strength is a problem which has wide implication in analysis of hazards posed by tailings dams, hydraulic fill dams, and literally all embankments which are considered susceptible to liquefaction. The problem has been considered by several workers with the aim of correlating post-liquefaction strength to pre-liquefaction soil data. Poulos *et.al.* (1985) related the post-liquefaction strength to the *in situ*, pre-liquefaction void ratio. Poulos' analysis was criticised by Seed (1987) who presented a new correlation of post-liquefaction strength with pre-liquefaction penetration resistance. Seed's correlation has since been superseded by a similar correlation by Stark and Mesri (1992). A comprehensive review of work in this area may be found in the paper by Stark and Mesri (1992).

None of the work discussed above suggests any dependence of strength on flow velocity despite the evidence that this may occur. Rouse (1984) noted that a velocity weakening effect is consistent with observations of exceptionally long run-outs noted for some flows. Ring shear tests on both soil and rock have also indicated strength-velocity dependence (Skempton,1985; Weeks,1993). These indications suggest that post-liquefaction strength may be far more dependent on conditions within the flow, and any correlation with pre-liquefaction characteristics may be weak or even non-existent.

The model developed here sets out to explore the possibility of velocity dependence. It is based on a plausible physical model for the flow and conceptually is very simple. Its mathematical representation is completely linear and nearly all the governing equations have closed form solutions. Nevertheless, the model describes a surprisingly rich variety of flow behaviour including both velocity strengthening and velocity weakening.

MODEL CONCEPT

The analytical model is illustrated in Figure 1. A sinusoidal slip surface separates a porous upper block of material from its rigid impermeable bed. The upper block is forced to slip at a constant velocity v_o. Full saturation is assumed, the top surface of the block being fully drained. One-

dimensional, vertical pore fluid flow is assumed. We denote the amplitude and wave length of the sinusoidal surface by a and l.

The model was motivated by an experiment described by Iverson and LaHusen (1989). They constructed a physical model composed of two arrays of fibreglass rods which could slide across each other to simulate slip on a rough surface. In each array the rods were fixed to allow a degree of permeability. After saturation with water, the upper array was pulled across the lower at a constant velocity. Measurements of dynamic pore fluid pressure were made near the slip surface. Iverson and LaHusen argued that the experimant could represent a segment of the slip plane found in a flow slide. Their results showed significant pore pressure variations at the slip surface and they suggested these might help explain how subaerial flows may exhibit extreme mobility.

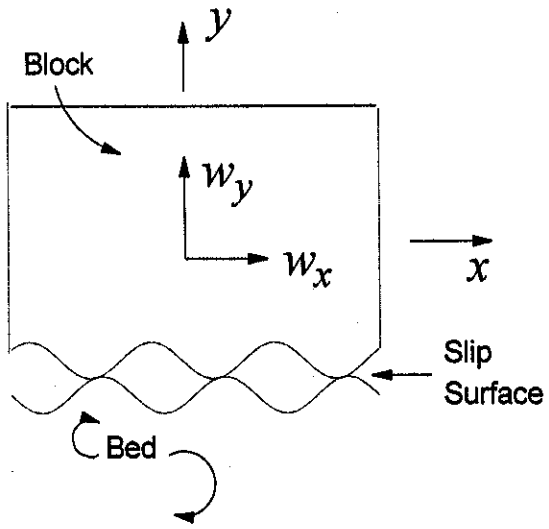

Figure 1. Schematic diagram of model.

As shown in Figure 1, the horizontal displacement of the flow is denoted by w_x. A second, more useful measure of horizontal motion is the relative displacement of the block with respect to the phase of the bed sinusoid. We will call this the phase displacement and denote it by ω. It is related to w_x and to l as follows

$$\omega = w_x \bmod l \qquad (1)$$

where mod denotes the modulo function. Thus as slip occurs ω increases from zero to l and is then reset to zero. When ω equals zero or l, the block is perfectly mated with the bed. The block need not be touching the bed however, depending upon the pore fluid stress.

We now expand this simple model to represent a large scale slip surface with random contact distribution. We can assume the large surface is composed of elements like that in Fig. 1, all with random phase displacements so that ω is uniformly distributed over the interval $[0,l]$. Each element slips with velocity v_o. The force required to maintain the velocity is clearly a function of ω, the phase displacement. Some elements may be separated due to high pore pressure on the slip surface, and the shear force on these will be zero. Other elements may be in contact, and the horizontal force will equal the frictional resistance based on the effective stress principle. The important point is this. If the phase displacements are uniformly distributed, then the average strength of the slip surface at the velocity v_o can be determined from the average strength of one element as slip occurs over one full phase (as ω increases from zero to l) and dividing that result by the wave length l. We will use this approach to assess the strength of the model.

EQUATIONS OF MOTION

The rough surface of the bed in Figure 1 is described by $a\sin(2\pi x/l)$. The lower surface of the moving block is $a\sin(2\pi(x-w_x)/l)$. The blocks may be in contact as shown in Fig. 1, or they may be separated when the block is buoyantly supported by the pore fluid. In either case, for any particular horizontal displacement w_x, there will be a corresponding minimum value for the vertical displacement w_y which is the minimum gap dimension, denoted b. If $w_y = b$ the blocks are in contact. The minimum gap dimension is most conveniently expressed in terms of the phase displacement ω.

$$b = 2a\sin(\pi\omega/l) \qquad (2)$$

Figure 2 shows b as a function of w_x. In many cases we will only need to consider one full phase of displacement as ω increases from zero to l. This corresponds to one of the humps shown in Figure 2.

Now suppose the mean depth of the sliding block is h, and assume h is large in comparison to a so that flow into or out of the block can be assumed vertical. The bed is taken as impermeable. The excess pore pressure will be denoted by u. Rigidity of the block implies a linear excess pore pressure

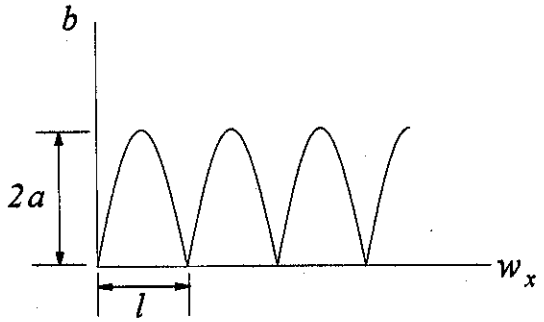

Figure 2. Minimum gap dimension b.

gradient. The value of u within the gap will depend upon the degree of dilatation or contraction of the slipping block, and upon the amount of flow into or out of the block. The rate of compressive straining of the pore fluid will be given by the velocity of the fluid particle located at the block surface divided by an appropriate gage length. The flow velocity at the block surface is given by Darcy's law as $-ku/\rho_w gh$ where k denotes the hydraulic permeability of the block and ρ_w is the pore fluid density. This velocity is measured relative to the vertical block velocity v_y. Thus the absolute velocity of the pore fluid at the block surface is $v_y + ku/\rho_w gh$. The strain rate is this velocity divided by a gage length which we take to be $2a$, the maximum value of b.. Finally, multiplying by the pore fluid bulk modulus κ , we obtain the rate of change of excess pore pressure

$$\dot{u} = -\frac{\kappa}{2a}\left(v_y + \frac{ku}{\rho_w gh}\right) \tag{3}$$

Equation (3) applies whether the block is in contact with the bed or not. The remaining equations depend upon the conditions of contact.

If the block is in contact with the bed, its vertical displacement and velocity are immediately found from

$$\begin{aligned} w_y &= b = 2a\sin(\pi\omega/l) \\ v_y &= \dot{w}_y = \frac{2\pi a v_o}{l}\cos(\pi\omega/l) \end{aligned} \tag{4}$$

Here the relationship $d\omega/dt = v_o$ has been used. Equations (3) and (4) completely describe the block motion and pore pressure so long as contact with the bed persists.

Next suppose the block is separated from the bed. Then instead of eqs. (4) we have

$$v_y = -(1-\rho_w/\rho)g + u/\rho h$$

which follows from Newton's law. Here ρ denotes the mass density of the sliding block. Note that the static pore pressure $\rho_w gh$ is included in this equation. Differentiating this result and using (3) gives the following expression for the motion of the block when separated from the bed

$$\ddot{v}_y + 2\eta\zeta\dot{v}_y + \eta^2 v_y = \frac{\kappa k}{2ah\rho}\left(\frac{\rho}{\rho_w} - 1\right) \tag{5}$$

Here

$$\eta^2 = \frac{\kappa}{2h\rho}, \text{ and } \zeta = \frac{k}{2\rho_w g}\sqrt{\frac{\kappa\rho}{2ah}}$$

We see that the block velocity obeys the equation of a damped harmonic oscillator. This results because the block is supported on a cushion of pore fluid, and flow into or out of the block provides a damping mechanism. It is a simple matter to integrate eq. (5) to determine both the velocity and the vertical displacement w_y.

Equations (3) through (5) describe the possible states of motion of the block. In a calculation we may change from one set of equations to another depending upon whether contact exists or not. If the blocks are separated, the criterion for contact is simply $w_y = b$. If the integration of eq. (5) suggests at any time that w_y is equal or less than the current minimum gap dimension b, then contact has occurred and the contact equations come into play. Conversely, if the block is in contact with the bed, the criterion for separation depends upon the value of u. If u equals or exceeds the critical excess pore pressure given by

$$u_s = (\rho - \rho_w)gh - 2\rho ha\left(\frac{\pi v_o}{l}\right)^2 \sin(\pi\omega/l) \tag{6}$$

then separation will occur. The value of u_s corresponds to the excess pore pressure which will produce an acceleration of the block greater than that caused by continued contact.

We can now visualise a typical cycle of motion of the block. Figure 3 shows the vertical displacement w_y (solid line) and the minimum gap dimension b (dashed line) over one full phase of horizontal displacement. Moving from left to right on the figure, the block is initially separated and is

drifting down towards the bed. Contact occurs at the point marked c. The block is then kinematically constrained to follow the bed contour, until at the point marked s separation occurs and the buoyant downward drift begins again. An interesting point arises here. The response of the block over this cycle is fully determined by the equations of motion together with initial values for the variables evaluated at $\omega = 0$. If the values of displacement, velocity and pore pressure at the end of the cycle are the same as those at the beginning, then the block will exactly repeat itself over the next cycle of slip as well as all succeeding cycles. This is called a limit cycle. When the slip velocity v_o is small or moderate, we find that limit cycle conditions exist and the block response repeats itself every full phase of the bed sinusoid. As the slip velocity increases, the limit cycle may lengthen to cover two or more phases of the bed sinusoid, and, at sufficiently high values of v_o, no limit cycle can be found and the motion is chaotic. These points will be considered below.

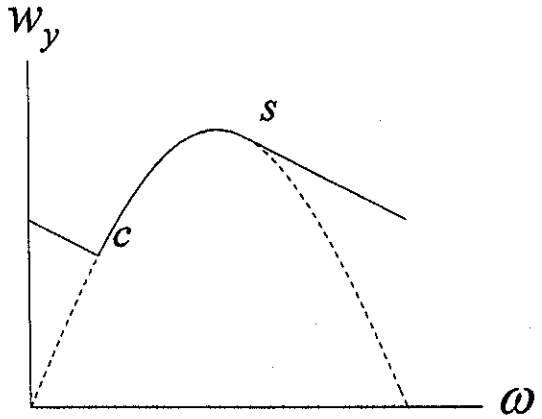

Figure 3. Motion during a typical cycle.

One other important point concerning the equations of motion should be noted here. Whenever the block is moving upwards, dilatation may result in negative excess pore pressures u. The total pore pressure will decrease, and, depending on the magnitude of the static pore pressure, we may find the total pore pressure approaches a value of negative one atmosphere. At this value cavitation may occur in the pore fluid (McManus and Davis, in press). The result is a lower limit on the excess pore pressure which we will denote as the cavitation pressure u_{cav}. If the value of u reaches u_{cav}, then the equations of motion must be appropriately altered by setting $du/dt = 0$. This may have a very significant effect on the block motion.

DETERMINATION OF STRENGTH

In order to assess the overall strength of the large slip surface we will consider the average strength of our block as it moves across one or more wave lengths of the bed sinusoid. First consider the case where a limit cycle of one wave length exists. Then we need only calculate the average strength over this interval.

Consider the forces acting on the block while in contact with the bed shown in Figure 4. Let the force required to produce a constant slip velocity v_o be f. We will define the frictional strength s_f as the work done by f in one full phase of motion divided by the wave length l.

$$s_f = \frac{1}{l}\int_0^l f \, d\omega \tag{7}$$

The value of f is zero if the block is separated from the bed, otherwise the force system in Figure 4 applies. The angle of dilatation δ is a function of the phase position

$$\delta = \tan^{-1}\left(\frac{2\pi a}{l}\cos\frac{\pi\omega}{l}\right) \tag{8}$$

The buoyant weight of the block is $(\rho - \rho_w)glh$. Its vertical acceleration is $-2a(\pi v_o/l)^2 \sin(\pi\omega/l)$. Equilibrium of forces then gives

$$f = \left\{-ul + (\rho - \rho_w)ghl + 2\rho hla\left(\frac{\pi v_o}{l}\right)^2 \sin\frac{\pi\omega}{l}\right\}\tan(\varphi + \delta) \tag{9}$$

Here φ denotes the intrinsic angle of friction of the material which composes the block and bed. When equation (9) is used in equation (7) the frictional strength can be determined for single limit cycle motions. If multiple limit cycles are found, equation (7) is easily generalised by extending the limits of integration.

Another source of strength in addition to the frictional strength is the impact strength s_i. Whenever the block contacts the bed, its kinetic energy is altered. Conventional theories of impact

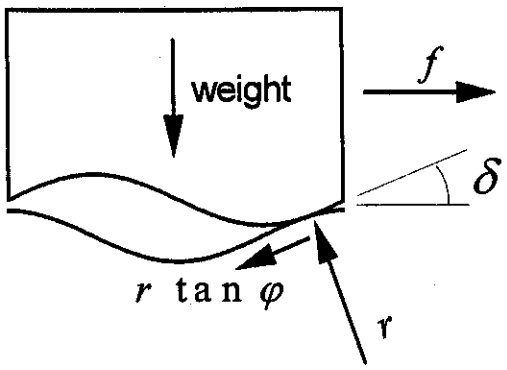

Figure 4. Forces acting while the block is in contact with the bed.

(Keller, 1986) relate the tangential impulse applied to the impacting object to the normal impuse by the coeffiecient of friction. Using the conventional theory we can determine for any impact the horizontal component of velocity which the block would have, post impact, were the constant velocity v_o condition not imposed. Let this velocity be denoted v_x^+. In general v_x^+ will be smaller than v_o. Thus energy is effectively dissipated in the impact. Another way of looking at this is to note that we must add energy to the block following any impact in order that the constant horizontal velocity v_o be maintained. The total dissipated kinetic energy summed over all impacts occurring in a cycle divided buy the wave length gives the second source of strength.

$$s_i = \frac{1}{2}\rho h \sum_{impacts}\left[(v_o)^2 - (v_x^+)^2\right] \qquad (10)$$

For high values of v_o this may be the most significant source of strength.

Finally we will define the effective angle of friction φ_{eff} in the obvious way

$$\varphi_{eff} = \tan^{-1}\left(s_f + s_i\right)/\left(\rho - \rho_w\right) ghl \qquad (11)$$

It is dependence of φ_{eff} on the slip velocity v_o which is the main focus of this work.

STRENGTH-VELOCITY DEPENDENCE

In this section we present a small selection of results. Limitations of space will not permit a complete discussion of the model response. Results presented will be condfined to the case where the separated motion of the block is overdamped ($\zeta \geq 1$). A range of slip velocities covering four orders of magnitude will be considered.

Values of the model parameters for the calculations shown below are summarised in Table 1. The value used for ρ is typical for moderately dense flows. The value for κ is the bulk modulus of water. The permeability would be typical for clean gravels or heavily fractured rock with relatively large particale sizes. The value of 10 *m* for *h* is arbitrary but flows of this depth are not uncommon. Note that *a* and *l* enter the calculation only through their ratio, which we take to be .067. This number correspondes to the interlocking dimension of a close packed array of uniform cylindrical rods divided by their centre to centre dimension. Finally, the intrinsic angle of friction is typical of a clean sand.

Table 1. Model parameter values.

Parameter	Value	Parameter	Value
a/l	.067	φ	24 deg
h	10 *m*	ρ	$1.75\ t/m^3$
k	$2\times10^{-3}\ m/s$	κ	$2.2\times10^{9}\ N/m^2$

Low Velocity Response

If the slip velocity is sufficiently small, the limit cycle response will exhibit continuous contact between the block and the bed. In this case the separated equations of motion never come into play, and there is no requirement for determining points of contact and separation.

For very small values of v_o the pore fluid has ample time to move into or out of the block without creating appreciable pore pressures. In the limit as v_o approaches zero, so must the excess pore pressure vanish. We can set u and v_o equal to zero in equation (9) and use the result to determine the low velocity strength limit. This gives

$$\varphi_o = \tan^{-1}\left[\frac{1}{\tan\varphi}\left(\frac{\tan^2\varphi + 1}{\sqrt{1-\left(2\pi a \tan\varphi/l\right)^2}} - 1\right)\right] \qquad (12)$$

We see that φ_o is greater than φ for all $a>0$.

There is a well defined upper limit for the slip velocity at which continuous contact can occur. Separation will first occur at the end of a cycle when

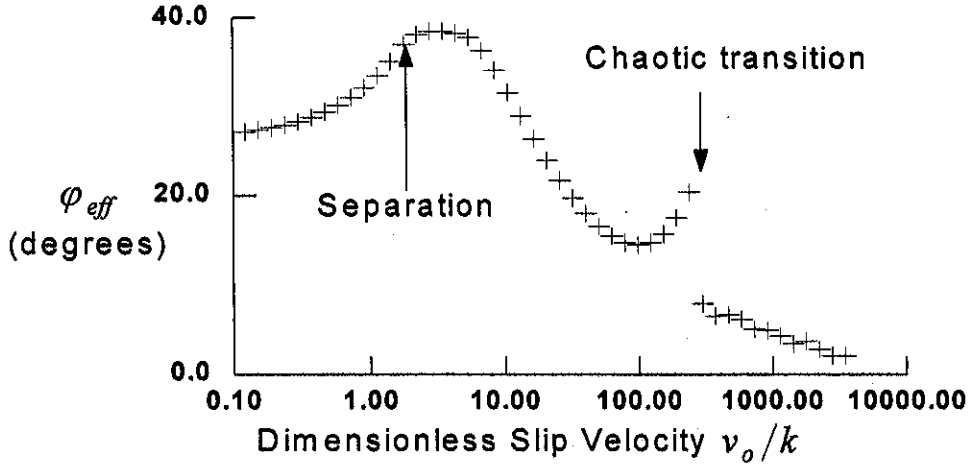

Figure 5. Strength-velocity response

.

$\omega = 1$. Setting $\omega = 1$ in equation (6) we see that the critical pore pressure for separation reduces to $u_s = (\rho - \rho_w)gh$. If we integrate (3) and set the result equal to u_s, we can find the upper limit on slip velocity for continuous contact. The exact result is somewhat complicated, but a close approximation which is much simpler is given by

$$\tilde{v}_o = (\rho - \rho_w) l\, k / 2\pi \rho a \qquad (13)$$

If the slip velocity v_o exceeds $\tilde{v}_o$, then for at least some part of the motion the block will be separated from the bed.

Low velocity response for the selected model parameters is shown in dimensionless form in Figure 5, to the left of the point marked 'separation'. As v_o increases from near zero the strength smoothly increases from the low velocity limit to a maximum value at the onset of separation.

Response at Moderate Slip Velocity

Next we consider the model strength over the central region of Figure 5. In this region the block undergoes some separation during each cycle. Single limit cycle response is maintained for nearly all velocities in this region.

Refering to the figure we see that shortly after separation commences the strength begins to decrease. Reasons for this are two-fold. Less contact between block and bed implies less opportunity for the block to generate frictional strength. A second reason is the onset of cavitation during contact. Cavitation limits the negative pore pressure and further inhibits development of frictional strength. In this region impacts are occurring, but the impact strength remains low for dimensionless slip velocities smaller than about 100. Once the slip velocity exceeds roughly 100 an increase in strength is apparent. This increase is entirely due to impact strength. The additional energy required to maintain a constant slip velocity begins to dominate the frictional energy dissipation in this region.

As we near a dimensionless slip velocity of roughly 250, the single limit cycle conditions noted at smaller velocities give way to multiple limit cycles. Then the strength abruptly drops to low values. This drop coincides with the onset of chaotic behaviour

High Velocity Behaviour

The abrupt drop in strength evident on Figure 5 occurs for a well defined reason. Whereas cavitation had occurred during contact with the bed at moderate slip velocities, it did not occur during separated motions. At high velocities this is not the case.

At first glance one might imagine that cavitation during separation will have little if any effect on the model strength. In fact it has a dramatic effect. When the block is separated from the bed and cavitation occurs, the forces acting to pull the block back down into contact are limited. The negative pore pressure which may occur during rapid separated motion acts to accelerate the block downward. Cavitation obviously limits this effect and promotes greater distances of free flight of the block. The block now maintains contact with the bed for only a brief period before it is thrown upward, passing over the peak of the bed sinusoid. Cavitation during this phase of the motion can only occur when the value of the separation pore pressure

u_s given in equation (6) is smaller than the cavitation pore pressure u_{cav}. Setting u_s equal to u_{cav} in equation (6), we can solve for the slip velocity at which separated cavitation may first occur. This gives

$$\hat{v}_o = \frac{l}{\pi}\left[\frac{(\rho - \rho_w)g - u_{cav}/h}{2a\rho}\right]^{1/2} \qquad (14)$$

For the model parameters used here, the value of $\hat{v}_o/k$ is 241, almost exactly the point at which the strength abruptly decreases. Once v_o exceeds $\hat{v}_o$, and cavitation is possible during separated motion, the entire behaviour of the model is radically altered.

As the slip velocity increases beyond $\hat{v}_o$ the characteristic limit cycle response observed before disappears. The trajectory of the block may pass over one or more peaks of the bed sinusoid, depending on the conditions at the previous impact. The absence of limit cycle behaviour is equivalent to chaos in a mathematical sense. For these higher slip velocities the determination of strength becomes more difficult than simply summing s_f and s_l over one or possibly two or three cycles. The high velocity data points shown in Figure 5 were calculated by summing the dissipated energy over a number of cycles ranging from 200 to 500, depending on the particular point, and finally dividing by the total distance of travel of the block (i.e. dividing by l times the number of cycles used). In each case a sufficiently large number of cycles was used so that a stable value of φ_{eff} was acheived.

DISCUSSION

The model presented here is clearly speculative, but it nevertheless possesses a number of interesting and possibly useful features. First it is a physical model in the sense that we can easily visualise its components. Second, its behaviour is relative easily determined, most of the equations being solvable in closed form. Third, its response shows characteristics which obsevations of real flows suggest may be physically possible in nature.

The strength-velocity relationship shown in Figure 5 offers two stable slip velocities. The first is very low velocity creep coreresponding to points near the left hand side of the figure. This might occur in situations where the low velocity strength limit φ_o is slightly exceeded. If, however, the loads acting on the flow are such that the peak strength near 36 degrees is exceeded, then the region of velocity softening is entered and unstable slip will occur until the velocity reaches the second stable value near v/k of roughly 100. If the system of loads acting on the flow is short lived, then stable slip will continue until the load drops beneath the corresponding stable strength value of roughly 14.5 degrees. On the other hand, if higher loads are maintained, then the slip velocity will continue to increase and unstable, high velocity flow will result. These are all features which have been observed in real flows.

REFERENCES

Iverson, R.M. and R.G. LaHusen 1989. Dynamic pore pressure fluctuations in rapidly shearing granular materials. *Science*. 246:796-799.

Johnson, A.M. 1984. Debris flow. in *Slope Instability*. eds D. Brunsden and D.B. Prior. New York: Wiley

Keller, J.B. 1986. Impact with friction. *J. Appl. Mech.* 53:1-4.

McManus, K.J. and R.O. Davis, in press. Dilation induced pore fluid cavitation in sands. *Geotechnique*.

Poulos, S.J., G. Castro and W.France. 1985. Liquefaction evaluation procedure. *J. Geotech. Engg. ASCE*. 111:772-792.

Rouse, W.C. 1984. Flowslides. in *Slope Instability*. eds D. Brunsden and D.B. Prior. New York: Wiley.

Seed, H.B. 1987. Design Problems in soil liquefaction. *J. Geotech. Engg. ASCE*. 113:827-845.

Skempton, A.W. 1985. Residual strength of clays in landslides, folded strata and the laboratory. *Geotechnique*. 35:3-18

Stark, T.D. and G. Mesri. 1992. Undrained shear strength of liquefied sands for stability analysis. *J. Geotech. Engg. ASCE*. 118:1727-1747.

Weeks, J.D. 1993. Constitutive laws for high velocity frictional sliding and their influence on stress drop during unstable slip. *J. Geoph. Res.* 98.B10:17637-17648.